

Ho^{3+} single-ion excitations in $\text{Y}_{0.99}\text{Ho}_{0.01}\text{Ba}_2\text{Cu}_3\text{O}_x$ ($6 < x < 7$)

This article has been downloaded from IOPscience. Please scroll down to see the full text article.

1999 J. Phys.: Condens. Matter 11 2921

(<http://iopscience.iop.org/0953-8984/11/14/008>)

View [the table of contents for this issue](#), or go to the [journal homepage](#) for more

Download details:

IP Address: 171.66.16.214

The article was downloaded on 15/05/2010 at 07:17

Please note that [terms and conditions apply](#).

Ho³⁺ single-ion excitations in Y_{0.99}Ho_{0.01}Ba₂Cu₃O_x (6 < x < 7)

W Henggeler[†], M Guillaume[†], P Allenspach[†], J Mesot[†], A Furrer[†] and M Adams[‡]

[†] Laboratory for Neutron Scattering, Eidgenössische Technische Hochschule Zürich and Paul Scherrer Institut, CH-5232 Villigen PSI, Switzerland

[‡] Rutherford Appleton Laboratory, Chilton, Didcot, Oxfordshire OX11 0QX, UK

Received 17 September 1998, in final form 29 December 1998

Abstract. We performed high-resolution inelastic neutron scattering experiments to examine the low-energy crystalline-electric-field (CEF) excitations of single Ho³⁺ ions in Y_{0.99}Ho_{0.01}Ba₂Cu₃O_x (6 < x ≤ 7). The observed magnetic response versus oxygenation exhibits a discrete character in energy which suggests the presence of different types of cluster for different doping levels. In the undoped sample (x = 6.14) we observe a splitting of the Γ₅ CEF level due to the exchange interaction between the Ho³⁺ ions and the antiferromagnetic subsystem of copper spins. For all the doped compounds we observe line asymmetries for which possible origins are discussed.

1. Introduction

Quite early in the study of high- T_c cuprate superconductors it was realized that rare-earth (R) ions can be introduced into the system without changing the superconducting transition temperature. Moreover, in contrast to conventional superconductors, a coexistence of superconductivity and long-range magnetic order of the R sublattice was discovered at low temperatures [1]. Subsequently there have been substantial efforts to achieve a detailed understanding of the low-energy electronic properties that define the magnetic ground state of the R ions. Relevant information has become available mainly through inelastic neutron scattering (INS) studies of the crystalline-electric-field (CEF) interaction at the R site [2].

The CEF interaction, however, is not only related to the magnetic properties, but may also lead to an improved understanding of the superconducting state. In particular, the temperature dependence of the line widths of CEF excitations provides information on the opening of the energy gap, the pseudogap and the order-parameter symmetry [3, 4]. In addition, since in most high- T_c compounds the R ions are situated close to the superconducting CuO₂ planes, the CEF interaction at the R site constitutes an ideal local probe of the charge distribution and thereby monitors directly changes of the carrier concentration induced by doping [5, 6]. Due to the local nature of the CEF interaction a separation into different local components, i.e., the formation of local regions or clusters of undoped, intermediately doped and highly doped character was observed [7, 8]. This phenomenon which may be called ‘frustrated phase separation’ has been observed by other local probes such as Mössbauer [9], NMR [10] and μ SR [11] experiments. For a critical volume fraction of 50% the doped clusters form a two-dimensional percolative network, and the system undergoes a transition from the insulating to the metallic state, in excellent agreement with the observed onset of superconductivity [7, 8].

A different type of structural and/or electronic inhomogeneity has been detected in the highly doped compounds. Several experiments suggest the presence of charge density waves or stripes in optimally doped samples like $\text{Bi}_2\text{Sr}_2\text{CaCu}_2\text{O}_{8+y}$ [12], $\text{La}_{1.85}\text{Sr}_{0.15}\text{CuO}_4$ [13], $\text{Nd}_{1.835}\text{Ce}_{0.165}\text{CuO}_4$ [14], $\text{YBa}_2\text{Cu}_3\text{O}_7$ [15], $\text{Tl}_2\text{Ba}_2\text{CaCu}_2\text{O}_8$ and $\text{La}_{1.85}\text{Ba}_{0.15}\text{CuO}_4$ [16]. In the $\text{YBa}_2\text{Cu}_3\text{O}_7$ compounds, EXAFS measurements also reveal the presence of two different Cu–O(apical) distances [17], indicating a local disorder of the CuO_2 planes.

An analysis of the line shape of the CEF excitations in $\text{HoBa}_2\text{Cu}_3\text{O}_x$ indicated that the appearance of inhomogeneities in the high-doping regime can as well be detected by CEF spectroscopy [18]. However, the presence of Ho–Ho interactions strongly influences the line shape of the CEF excitations and makes such an analysis quite delicate, even at Ho concentrations as low as 10% [3, 19, 20]. To handle this problem, we performed INS experiments on highly diluted $\text{Y}_{0.99}\text{Ho}_{0.01}\text{Ba}_2\text{Cu}_3\text{O}_x$ compounds, prepared by the sol–gel technique, and thereby avoided a clustering of the Ho^{3+} ions. We focused on the lowest-lying CEF excitation in order to achieve the highest possible energy resolution.

2. Experiment

We prepared samples of $\text{Y}_{0.99}\text{Ho}_{0.01}\text{Ba}_2\text{Cu}_3\text{O}_x$ by the sol–gel technique as follows. The nitrates $\text{Ho}(\text{NO}_3)_3 \cdot 5\text{H}_2\text{O}$, $\text{Y}(\text{NO}_3)_3 \cdot 4\text{H}_2\text{O}$, $\text{Ba}(\text{NO}_3)_2$, $\text{Cu}(\text{NO}_3)_2 \cdot x\text{H}_2\text{O}$ and a 50 mol% excess of solid citric acid were dissolved in water. After adding a 50 mol% excess of ethylene glycol ($\text{C}_2\text{H}_6\text{O}_8$) the solution was put on a heater/mixer plate ($<100^\circ\text{C}$) until H_2O evaporated and nitrates+citric acids reacted, forming a blue gel. The gel was then put into Al_2O_3 crucibles and dried on a heater plate. The crucible was transferred to a furnace and heated up to 300°C for 12 hours and then to 500 and 700°C for 2 h each. After cooling, grinding the powder and making pellets, the samples were sintered at 900°C for 24 h with constant oxygen flow. After oxygen reduction, we determined the superconducting transition temperature T_c by measuring the zero-field susceptibility. The $x = 6.98$, $x = 6.86$ and $x = 6.79$ samples showed superconducting transition temperatures of 93 ± 1 , 92 ± 1 and 90 ± 2 K, respectively, whereas the $x = 6.70$ and $x = 6.65$ samples showed a T_c of 63 ± 2 and 59 ± 2 K, respectively. No superconducting transition above 20 K was observed for the $x = 6.45$ and of course for the $x = 6.14$ sample. The samples were characterized by neutron diffraction techniques and turned out to be nearly single phase, with small traces (<2 wt%) of the green phase, probably due to nonstoichiometry. For the structure investigations we used the diffractometer D1A at the high-flux reactor of the Institute Laue–Langevin (ILL) at Grenoble. The Rietveld refinement of these data allowed the determination of the oxygen content x with an error $\Delta x = 0.03$. In all orthorhombic compounds about 14% of the O(5) positions were found to be occupied. The INS experiments were performed on the high-resolution indirect geometry spectrometer IRIS [21], installed at the pulsed spallation neutron source ISIS of the Rutherford Appleton Laboratory at Chilton, UK. We used a cooled pyrolytic graphite (002) analyser close to back-scattering geometry which gives an energy resolution of $25 \mu\text{eV}$. The raw data have been calibrated according to standard procedures.

3. Results

Figure 1 (upper part) shows the energy spectrum observed for $\text{Y}_{0.99}\text{Ho}_{0.01}\text{Ba}_2\text{Cu}_3\text{O}_{6.98}$. Besides the intense elastic line there is a sharp spike at around 0.25 meV, which is an instrumental artifact due to fast neutrons. A well defined inelastic line shows up at 0.5 meV that corresponds to the lowest-lying CEF transition $\Gamma_3\text{--}\Gamma_4$ of the Ho^{3+} ions [6] which is of course not present

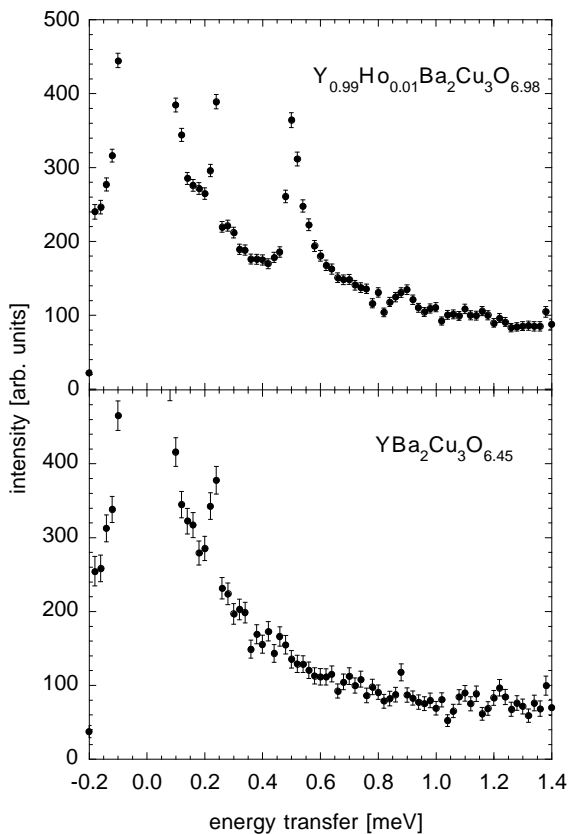


Figure 1. Energy spectra of neutrons scattered from YBa₂Cu₃O_{6.45} and Y_{0.99}Ho_{0.01}Ba₂Cu₃O₇. $T = 1.5$ K, scattering angle $29.9^\circ \leq \phi \leq 156.6^\circ$, analyser energy $E_a = 1.82$ meV.

in the energy spectrum observed for YBa₂Cu₃O_{6.45}, see the lower part of figure 1. In the further treatment of the data we have used the YBa₂Cu₃O_{6.45} spectrum to determine the non-magnetic scattering contributions, which are structureless and gradually fall with increasing energy transfer, thus the purely magnetic scattering from the Ho³⁺ ions was obtained by taking the normalized differences of the energy spectra observed for the Ho doped samples and the YBa₂Cu₃O_{6.45} sample. The result of this procedure is shown in figure 2. The magnetic scattering of the Ho³⁺ ions shows the following behaviour for different doping levels. For $x = 6.98$ we observe the Γ_3 – Γ_4 CEF excitation at 0.5 meV. The line has a pronounced tail at the high energy side. While the peak position remains at 0.5 meV for $6.79 \leq x \leq 6.98$, it is shifted to higher energies for $x = 6.70$, in agreement with the results obtained for undiluted HoBa₂Cu₃O_x [6]. For the samples with oxygen content $6.14 < x < 6.98$ the magnetic scattering has a similar asymmetric shape as in the $x = 6.98$ compound; however, the linewidth gradually increases with decreasing oxygen content x . For the $x = 6.14$ sample we observe two lines at ~ 1.0 meV and ~ 1.1 meV. We therefore used the following procedure to fit the spectra. First a flat background was included. The asymmetric scattering function of the $x = 6.98$ compound was described by a Lorentzian centred at an energy transfer E which was cut off to zero below E . The half width at half maximum of the truncated Lorentzian function was $60 \mu\text{eV}$. This description is of course arbitrary but it provides a good fit of the

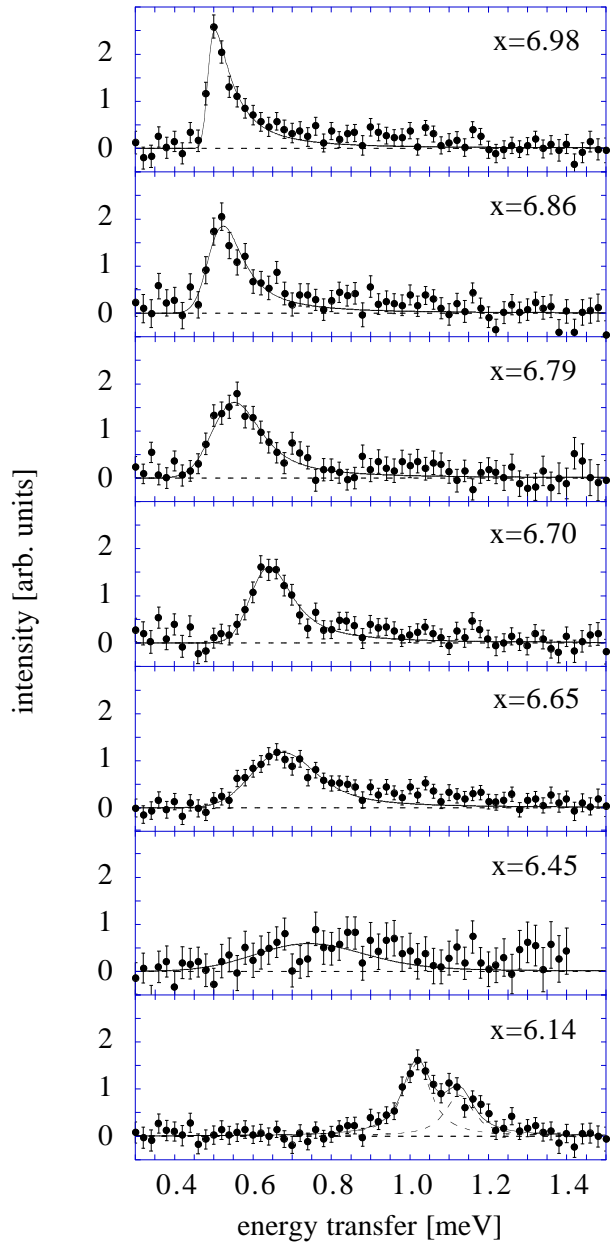


Figure 2. Energy spectra of neutrons scattered from $\text{Y}_{0.99}\text{Ho}_{0.01}\text{Ba}_2\text{Cu}_3\text{O}_x$ ($6.14 \leq x \leq 6.98$) taken at $T = 1.5$ K. The data correspond to the difference of the energy spectra observed for the Ho-doped samples and the $\text{YBa}_2\text{Cu}_3\text{O}_{6.45}$ sample. The lines are the results of fits as explained in the text.

magnetic response. The true scattering function might be different and will be discussed in section 4. To describe the broader magnetic response of the $6.14 < x < 6.98$ samples this line was then convoluted with a Gaussian. Finally, to obtain the scattering function, the lines were moreover convoluted with the resolution function. For the undoped compound ($x = 6.14$) we used two Lorentzian lines convoluted with the resolution function. Due to the excellent

resolution (25 μeV) of the IRIS spectrometer, the convolution with the resolution curve has only a very small influence and therefore the observed spectra directly show the magnetic response of the systems.

This description of the line shapes fits the spectra quite well (figure 2). The convolution of two different functions (truncated Lorentzian and Gaussian) reflects the fact that we have two different mechanisms which lead to a line broadening. To see whether this line description is reasonable, we furthermore tested it for the Y_{0.9}Ho_{0.1}Ba₂Cu₃O₇ compound. In this sample, due to Ho–Ho dimer splitting, there is a superposition of one monomer and two dimer excitations [3, 19]. In figure 3 it is shown that these three excitations are very well described by exactly the same truncated Lorentzian as used in the description of the Y_{0.99}Ho_{0.01}Ba₂Cu₃O₇ sample. However, dimer–dimer, monomer–dimer and monomer–monomer interactions lead to additional dispersions of the CEF excitations, which we can describe by a convolution of these lines with an additional Gaussian function of width $\sim 30 \mu\text{eV}$.

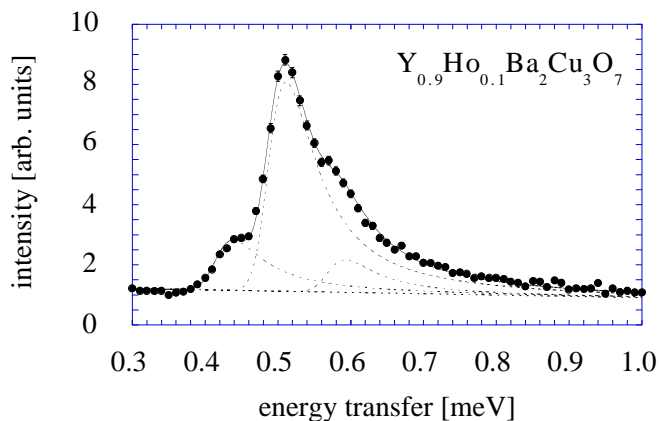


Figure 3. Energy spectra of neutrons scattered from Y_{0.9}Ho_{0.1}Ba₂Cu₃O₇. $T = 1.5 \text{ K}$, scattering angle $29.9^\circ \leq \phi \leq 156.6$, analyser energy $E_a = 1.82 \text{ meV}$.

4. Data interpretation

There are several known mechanisms which lead to a broadening of CEF lines. On one hand there is the interaction between different CEF excitations. This interaction is not present in our case because of the high dilution of the Ho³⁺ ions. On the other hand there is the interaction of the CEF levels with the conduction electrons and the phonons. The resulting broadening, however, can be neglected at low temperatures [3, 4]. Moreover, these interactions lead to a symmetric broadening of the lines. In our case however, the line broadening is highly asymmetric. This can only be explained by the presence of different local environments at the rare-earth sites which leads to different crystal-field splitting energies for the Ho³⁺ ions.

Our data suggest that there are two different types of line broadening mechanism present in our samples. The first mechanism is best visible for the $x = 6.98$ compound, where it leads to an asymmetric broadening which can be described by the truncated Lorentzian mentioned earlier. The second mechanism leads to a broadening of Gaussian shape. The magnetic response is then the result of a convolution of both these two functions and of the resolution function. The second broadening mechanism is not relevant in the $x = 6.98$ compound, where the corresponding Gaussian line is smaller than the resolution function. It becomes however relevant for all other doped compounds. These two mechanisms seem to be independent.

They might be effective on different time-and/or length-scales. We will try to give a possible explanation for these two line broadening mechanisms.

As demonstrated in detail for $\text{RBa}_2\text{Cu}_3\text{O}_x$ [5, 6], the crystal-field interaction is mainly determined by the position and the charges of the oxygen ions in the CuO_2 planes. At $x = 6.14$ the system is an antiferromagnetic insulator. The oxygen environment of the Ho^{3+} ions is of tetragonal symmetry. Because the compound is nearly stoichiometric, the local environment of the rare-earth ion is well defined. The double-peak structure observed at around 1.05 meV is characteristic of the magnetic response of the Ho^{3+} ion in the undoped phase. It has been explained in terms of a splitting of the first excited Γ_5 doublet state due to Cu spin-wave excitations, as observed and analyzed in detail for $\text{Y}_{0.9}\text{Ho}_{0.1}\text{Ba}_2\text{Cu}_3\text{O}_x$ [20]. Our results are consistent with this interpretation; in particular, the splitting does not originate in any Ho–Ho interaction which could have still been present for a 10% Ho concentration.

In the case of $x = 6.98$, the oxygen environment of the Ho^{3+} ions is of orthorhombic symmetry, where the first excited doublet present in the $x = 6.14$ compound is split into two excited singlet states at ~ 0.5 meV and ~ 1.8 meV above the singlet ground state. It can be seen that the broadening of the line at 0.5 meV towards the low-energy side is very small and corresponds to the instrumental resolution. This means that the configuration which leads to the magnetic response at 0.5 meV produces a sharp CEF excitation ($\Delta E < 25 \mu\text{eV}$) with a long relaxation time ($\tau \sim h/\Delta E > 2 \times 10^{-10}$ s). The pronounced broadening of the line on the high-energy side, however, indicates that besides the CEF environment associated with the line at 0.5 meV there exist a number of other CEF environments leading to lines at energies > 0.5 meV. Obviously there exist structural and/or charge inhomogeneities in the superconducting planes even in the optimally doped $x = 6.98$ compound.

A possible explanation for such inhomogeneities could be a charge modulation on the oxygen sites in the copper oxide planes, i.e. the presence of charge stripes. Such a modulation would result in several different CEF surroundings for the Ho ions, leading to a wide distribution of excitation energies. However, it is not straightforward to see why the resulting lineshape would be asymmetric. Moreover, there is no experimental evidence for the existence of charge stripes in the $\text{RBa}_2\text{Cu}_3\text{O}_x$ compounds so far.

An alternative explanation for the line asymmetry could be associated with the 14% occupation of the O(5) positions in the chains. For a Ho^{3+} ion with all the four surrounding O(4) positions as well as all the four surrounding O(5) positions empty (0.2% probability), the local CEF environment is tetragonal, thus the singlets at 0.5 meV and 1.8 meV are merged to a doublet at about 1 meV. On the other hand, for Ho^{3+} ions with no surrounding O(5) positions but all surrounding O(4) positions occupied (30% probability) which corresponds to a local CEF environment of orthorhombic symmetry, the CEF excitation will lie at 0.5 meV. For all other cases ($\approx 70\%$ probability), the CEF excitations consecutively occur in the energy range from 0.5 to 1 meV with diminishing amplitude. A superposition of all these excitations will then produce an asymmetric lineshape. At present we strongly favour this explanation which is furthermore supported by similar observations of line asymmetry for the lowest CEF excitation in $\text{Ho}_{0.1}\text{Y}_{0.9}\text{Ba}_2\text{Cu}_3\text{O}_7$ [3] as well as for the three lowest CEF excitations in $\text{HoBa}_2\text{Cu}_3\text{O}_{6+x}$ ($x > 0.4$) [6].

For all the intermediately doped compounds, there is moreover a second mechanism which leads to a symmetric line broadening that we describe by a Gaussian line. This mechanism seems to coexist with the mechanism that leads to the asymmetric line broadening. As this second mechanism is absent in the $x = 6.98$ compound, we can again exclude that it has its origin in the interaction of phonons or electrons with the CEF excitation. We will demonstrate that this broadening can be explained in the same terms as the line broadening of the Er CEF excitations in $\text{ErBa}_2\text{Cu}_3\text{O}_x$ ($6 < x < 7$) [7].

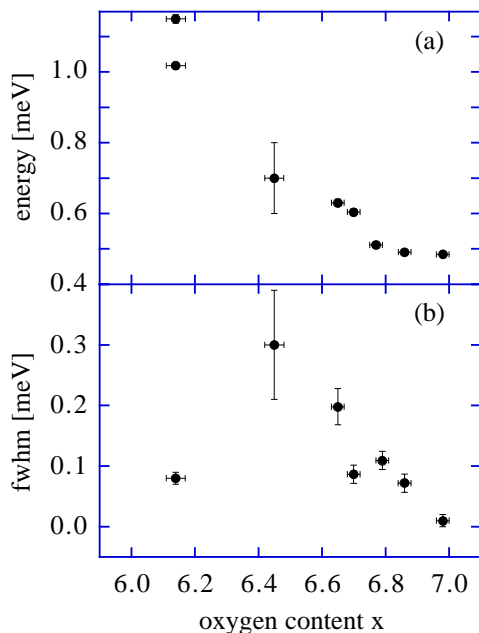


Figure 4. (a) Energies corresponding to maximum magnetic scattering of neutrons from Y_{0.99}Ho_{0.01}Ba₂Cu₃O_x ($6.14 \leq x \leq 6.98$). (b) Full width at half maximum of the magnetic scattering of neutrons from Y_{0.99}Ho_{0.01}Ba₂Cu₃O_x ($6.14 \leq x \leq 6.98$).

In figure 4 we show the positions of the peak maxima and the fwhms of the Gaussian lines for the different oxygen contents. The energies of the maxima increase from 0.5 meV for $x = 6.98$ to 1.1 meV for $x = 6.14$. The increase of the energies with oxygen content is not really smooth but displays rather a discrete behaviour, with energies centred around 0.5 meV, 0.65 meV and ≈ 1 meV. As expected, the smallest linewidths and therefore the most homogeneous configuration are visible in the spectra of the fully doped ($x = 6.98$) and undoped ($x = 6.14$) compounds. For all the intermediately doped compounds, the linewidths are broader. These observations agree with the doping picture which has been established for ErBa₂Cu₃O_x with help of neutron scattering experiments [7]. For $x = 6.14$ the system is an antiferromagnetic insulator; the double-peak structure observed at around 1 meV is characteristic of the magnetic response of the Ho³⁺ ion in the undoped tetragonal phase. Upon increasing x , i.e. when adding oxygen ions into the chains, holes are transferred into the CuO₂ planes giving rise to intermediately doped clusters with the characteristic magnetic response of the Ho³⁺ ions being the line at 0.65 meV. For the samples with oxygen content $6.45 \leq x \leq 6.70$ these clusters dominate the magnetic response; however, they coexist with clusters that correspond to other doping levels. The dominating clusters are therefore not fully homogeneous and the magnetic response is broadened. More specifically, line broadening is due to structural inhomogeneities and gradients in the charge distribution which occur predominantly at the border lines between different cluster types [18]. This is nicely demonstrated for the $x = 6.45$ sample where the magnetic response of the dominating intermediately doped clusters is so broad that it is at the limit to be detected. By going from oxygen content $x = 6.45$ to $x = 6.70$, these dominating clusters grow in size and therefore become more and more homogeneous. This is directly reflected in the changes of the linewidths of the magnetic response in these samples (figure 4(b)). Upon further increasing the

hole concentration a new type of highly doped cluster is formed which dominates the magnetic response of the Ho^{3+} ions at high doping ($x \geq 6.79$, line at 0.5 meV). Again, by going from $x = 6.79$ to $x = 6.98$ these clusters become bigger and more homogeneous.

5. Conclusion

High-resolution neutron spectroscopy was applied to study the low-lying CEF excitations of Ho^{3+} ions in $\text{Y}_{0.99}\text{Ho}_{0.01}\text{Ba}_2\text{Cu}_3\text{O}_x$ ($6 < x < 7$). Due to the local character of the CEF interaction and the excellent resolution of the instrument we were able to monitor directly the evolution of the different types of local region versus oxygenation. Our results confirm the idea of frustrated phase separation and of the inhomogeneous character of the superconducting state. The size of the clusters is directly reflected in the symmetric line broadening of the CEF excitations. A second type of line broadening mechanism that leads to an asymmetric line in the doped compounds shows an inhomogeneity of the CuO_2 planes that can be explained most probably by a superposition of CEF excitations due to the statistical distribution of oxygen ions at the O(5) sites.

Acknowledgments

Financial support by both the Swiss National Science Foundation and the Bundesamt für Bildung und Wissenschaft is gratefully acknowledged.

References

- [1] Dunlap B D et al 1987 *J. Magn. Magn. Mater.* **68** L139
- [2] Furrer A 1993 *Selected Topics in Superconductivity* ed L C Gupta and M S Multani (Singapore: World Scientific) p 349
- [3] Boothroyd A T, Mukherjee A and Murani A P 1996 *Phys. Rev. Lett.* **77** 1600
- [4] Mesot J, Böttger G, Mutka H and Furrer A 1998 *Europhys. Lett.* **44** 498
- [5] Mesot J, Allenspach P, Staub U, Furrer A, Mutka H, Osborn R and Taylor A 1993 *Phys. Rev. B* **47** 6027
- [6] Staub U, Mesot J, Guillaume M, Allenspach P, Furrer A, Mutka H, Bowden Z and Taylor A D 1994 *Phys. Rev. B* **50** 4068
- [7] Mesot J, Allenspach P, Staub U, Furrer A and Mutka H 1993 *Phys. Rev. Lett.* **70** 865
- [8] Henggeler W, Cuntze G, Klauda M, Mesot J, Furrer A and Saemann-Ischenko G 1995 *Europhys. Lett.* **29** 233
- [9] Hodges J A, Bonville P, Imbert P and Jéhanno G 1991 *Physica C* **184** 259
- [10] Teplov M A, Bakharev O N, Dooglav A V, Egorov A V, Eremin M V, Tagirov M S, Tagirov A G, Volodin A G and Zhdanov R S 1991 *Physica C* **185–189** 1107
- [11] Niedermayer C, Bernhard C and Budnick J I 1995 *J. Magn. Magn. Mater.* **140–144** 1287
- [12] Bianconi A 1994 *Physica C* **235–240** 269
- [13] Bianconi A, Saini N L, Lanzara A, Missori M, Rossetti T, Oyanagi H, Yamaguchi H, Oka K and Ito T 1996 *Phys. Rev. Lett.* **76** 3412
- [14] Billinge S J L and Egami T 1993 *Phys. Rev. B* **47** 14 386
- [15] Egami T, Sendyka T R, Dmowski W and Louca D 1994 *Physica C* **235–240** 1229
- [16] Egami T, Toby B H, Billinge S J L, Janot C, Jorgensen J D, Hinks D G, Crawford M K, Farneth W E and McCaroon E M 1991 *High Temperature Superconductivity: Physical Properties, Microscopic Theory and Mechanisms* ed J Ashkenazi (New York: Plenum) pp 389–99
- [17] Mustre de Leon J, Conradson S D, Batistic I, Bishop A R, Raistrick I D, Aronson M C and Garzon F H 1992 *Phys. Rev. B* **45** 2447
- [18] Furrer A, Allenspach P, Fauth F, Guillaume M, Henggeler W, Mesot J and Rosenkranz S 1994 *Physica C* **235–240** 261
Mesot J and Furrer A 1994 *Physica C* **235–240** 1639
- [19] Guillaume M, Staub U, Fauth F, Mesot J, Furrer A and Carlile C J 1994 *Physica C* **223** 333
- [20] Aristov D N, Maleyev S V, Guillaume M, Furrer A and Carlile C J 1994 *Z. Phys. B* **95** 291
- [21] Carlile C J and Adams M A 1992 *Physica B* **182** 511